

Adsorption of Congo Red Dyes Using Mesoporous Silica MCM-48

Faridatun Sholehah¹⁾, Paulina Taba^{2,a)}, Yusafir Hala² and Bahrnun¹⁾

¹Master Program, Department of Chemistry, Faculty of Mathematics and Natural Sciences, Physical Chemistry Lab. Hasanuddin University, Perintis Kemerdekaan Street Km. 10 Tamalanrea, Makassar 90245, Indonesia.

²Department of Chemistry, Mathematics and Natural Sciences Faculty, Hasanuddin University, Perintis Kemerdekaan Street Km. 10 Tamalanrea, Makassar 90245, Indonesia.

^{a)} Corresponding author: paulinataba@unhas.ac.id

Abstract. Research on the synthesis of mesoporous silica (MCM-48) has been carried out by utilizing MCM-48 as an adsorbent for congo red (CR) dye. MCM-48 was synthesized hydrothermally using ludox HS40 as a silica source, CTAB and Triton X-100 as a template. Characterization was performed using Fourier Transform Infra-Red (FTIR) spectroscopy and Scanning Electron Microscope (SEM). The results showed that the optimum adsorption time of congo red by MCM-48 was 25 minutes. The adsorption capacity was determined by carrying out adsorption at various concentrations at the optimum time. Adsorption isotherms were determined using Langmuir and Freundlich adsorption isotherms with the adsorption capacity of MCM-48 of 185,185 mg/g. Through kinetics experiments that the adsorption process follows the pseudo-second-order kinetics equation model. This study shows that mesoporous carbon can be recommended as a good adsorbent.

INTRODUCTION

Pollution caused by toxic and hazardous chemicals has become a serious global problem and is assumed to worsen in the next few years. This is directly proportional to the number of manufacturing industries [1]-[2]. This industry uses dyes to color products in large volumes so that the demand for dyes increases exponentially. As a result, the massive production and use of colored substances such as synthetic dyes have increased. This cannot be avoided due to the use of synthetic dyes which are cheap, durable and easy to obtain [2]-[3]. Synthetic dyes are generally made from azo compounds and their derivatives from the benzene group. Congo red (CR) is an example of azo dyes with a very stable structure making it difficult to degrade. Therefore we need an effective way to remove the dye [4]-[6].

Methods that have been used to treat the problem of dye removal in wastewater such as photocatalytic [7], nanofiltration [8] and adsorption [2],[5]-[6] have been applied to remove dyes from aquatic systems. The adsorption method is a technique that is more efficient because of its flexibility, simplicity, cheapness and effectiveness [9]-[10]. The most important thing in the adsorption process is adsorbent. The synthesized adsorbent has the advantage because it can be made with a certain pore size according to need so that it will be more effective in its use as an adsorbent [11]-[12].

Mesoporous silica has attracted the attention of researchers since the discovery of the molecular sieves mesopore (M41S), M41S is divided into three types, namely MCM-41, MCM-48 and MCM-50. MCM-48 is widely used because it has a three-dimensional channel that allows particles to easily enter the material because the pores are not limited to one direction only so that blocking by other molecules can be avoided. The removal of some of the surfactants will be carried out by washing with HCl-ethanol to obtain porous adsorbents. The surfactants used were cetyltrimethylammonium bromide (CTAB) and Triton X-100. Cetyltrimethylammonium bromide (CTAB) is a

cationic surfactant and Triton X-100 is a neutral surfactant [13]-[17]. Based on the description above, this study was conducted to synthesize MCM-48 which is used as a congo red (CR) dye adsorbent.

MATERIALS AND METHODS

Materials

The materials for this study were Congo Red, Ludox HS40, cetyl trimethyl ammonium bromide (CTAB, Aldrich), triton X-100 (Sigma) as a surfactant, NaOH (sodium hydroxide), HCl (hydrochloric acid), ethanol, acetic acid (CH₃COOH), Whatman No.42 filter paper, distilled water and universal pH paper.

Equipment

The equipment used in this research is a thermometer, hotplate stirrer, analytical balance (Shimadzu AW220), magnetic stirrer (Fisher type 115), vacuum pump (type ME4C), Buchner filter, oven (SPNISOSFD type), UV-Vis spectrophotometer (Spektronik 20 D+), SEM (Scanning Electron Microscope), Spectrophotometer FT-IR Prestige-21 (Shimadzu).

Procedures

Synthesis of Mesoporous Silica MCM-48

The synthesis of MCM-48 was carried out using the method that has been done [15] which has been modified [18]. The surfactant was removed from the white product by washing HCl-ethanol one time and washing HCl-ethanol twice. Mesoporous silica MCM-48 as much as 1 gram was washed with 25 mL of 0.1 M HCl in 50% ethanol solution while stirring for 30 minutes at room temperature, then filtered, the precipitate was washed with distilled water until neutral pH and dried at 373 K. The same for the next wash [18].

Batch Adsorption Equilibrium Experiments

Batch adsorption experiments were carried out to evaluate the effect of contact time and concentration of the congo red solution. MCM-48-TC, MCM-48-C1 and MCM-48-C2 have weighed as much as 100 mg put into an erlenmeyer containing 50 mL of Congo red 300 mg/L solution. Then the mixture is stirred with a magnetic stirrer for 3 minutes and then filtered. The experiment was repeated with variations in the stirring time, respectively 5, 7, 10, 15, 20, 25, 30, 35 and 40 minutes and was done in triplo. The absorbance of the filtrate was measured using a UV-Vis spectrophotometer at its maximum wavelength ($\lambda_{max} = 496 \text{ nm}$) (obtained experimentally by us).

Then carried out variations in the concentration of the dye congo red (CR). A total of 100 mg of MCM-48 TC, MCM-48 C1 and MCM-48 C2 were added respectively to the erlenmeyer containing 50 mL of dye solution with various concentrations of 350, 400, 450, 500, 600, 700, 800 and 900 mg/L, then stirred using a magnetic stirrer for the optimum time. The mixture was filtered using Whatman no. 42 and measured using a UV-Vis spectrophotometer at the maximum wavelength (the experiment was carried out in triplo). The amount of dye adsorbed (mg) per gram of mesoporous silica adsorbent (MCM-48) was determined using Equation (1).

$$\frac{x}{m} = \frac{C_o - C_e}{W} V \quad (1)$$

where $\frac{x}{m}$ is the amount of dye adsorbed (mg/g), C_o is the concentration of the dye before adsorption (mg/L), C_e is the concentration of the dye after adsorption (mg/L), V is the volume of the dye solution (L) and W is the amount of mesoporous silica adsorbent (MCM-48) (g) [5]. The adsorption capacity can be determined using the Langmuir and Freundlich equations as in Equations (2) and (3).

$$\frac{C_e}{q_e} = \frac{1}{Q_0 b} + \frac{C_e}{Q_0} \quad (2)$$

$$\left(\log \left(\frac{x}{m}\right)\right) = \log k + \left(\frac{1}{n}\right) \log C_e \quad (3)$$

By plotting $\log \frac{x}{m}$ against $\log C$ for the Freundlich equation or C_e/Q_e against C_e for the Langmuir equation.

The Freundlich equation intercepts the k value (a parameter related to the adsorption capacity) and from the slope of the Langmuir equation, the Q_0 value associated with the adsorption capacity can be obtained [19]-[20].

RESULTS AND DISCUSSION

Research data relating to the synthesis of MCM-48 and its application as a waste adsorbent for congo red dyes are discussed, mesopore silica (MCM-48) is produced from synthesis using ludox HS40 as a source of silica, CTAB and Triton X-100 as surfactants, distilled water as a solvent and NaOH as a base catalyst to produce a white powder. Mesoporous silica (MCM-48) is then washed with HCl-ethanol to remove some of the surfactants and is used to adsorb the congo red dye. The adsorption of the congo red dye was done with time variations to obtain the optimum adsorption time. The optimum conditions were used to determine the adsorption capacity of the congo red dye by MCM-48. The characterization of the results of mesoporous silica synthesis (MCM-48) was carried out using FTIR and SEM instruments.

Characterization of Mesoporous Silica (MCM-48)

Characterization using SEM at a magnification of 3000 and 5000 times was carried out to observe the surface morphology of MCM-48 which is shown in Figure 1. The surface morphology appears rough with nearly spherical or elliptical particles as separate grains, this is due to the presence of pores and almost uniform pore size. After the surfactant is removed from the silica, a cavity containing silanol (Si-OH) groups will be formed. This is due to washing using HCl-ethanol which functions to remove the surfactant so that it has a large surface area [17], [21]-[22].

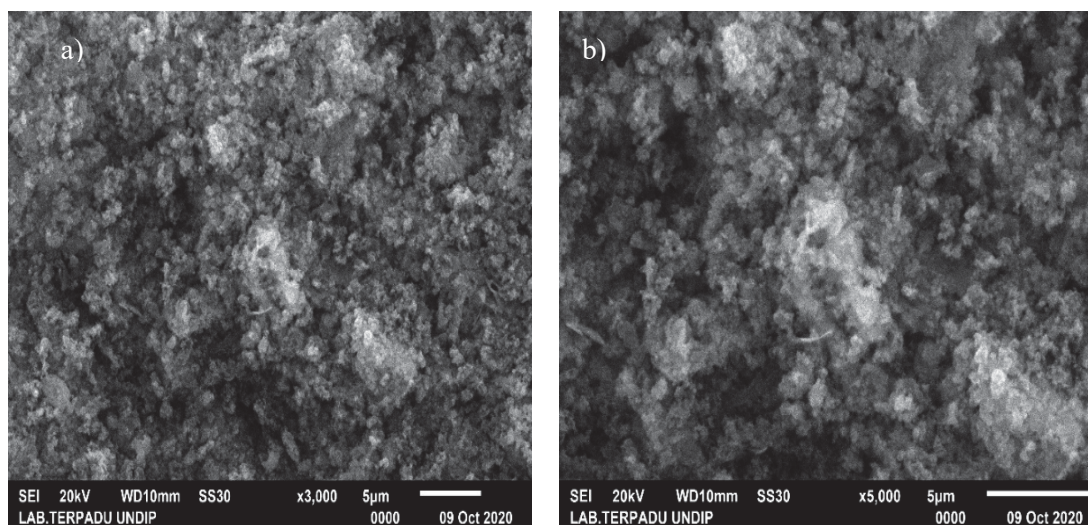


FIGURE 1. SEM images of MCM-48 a) 3000 times, and (b) 5000 times

The infrared spectrum of MCM-48 in Figure 2 shows the symmetrical stretching vibration of Si-O-Si in the absorption band with a wavenumber of 804 cm^{-1} and is supported by the bending vibration of Si-O-Si in the absorption band of 466 cm^{-1} . The weak absorption band given at wave number 964 cm^{-1} is the stretching vibration of Si-O and Si-OH. The 1095 cm^{-1} and 1229 cm^{-1} strong absorption bands are the asymmetric stretching vibrations of

Si-O-Si. The low C-H vibration was seen in the 1463 cm^{-1} absorption band. The stretched C-H vibration seen at wave number 2856 cm^{-1} shows the symmetric $-\text{CH}_2$ and $-\text{CH}_2$ antisymmetric functional groups at 2926 cm^{-1} which are the spectrum of the surfactant. The wide peak in the area of wave number 3475 cm^{-1} is the stretching vibration of $-\text{OH}$. These peaks are the result of hydroxyl groups and water being physically adsorbed by the MCM-48 mesoporous silica [20], [23]-[24].

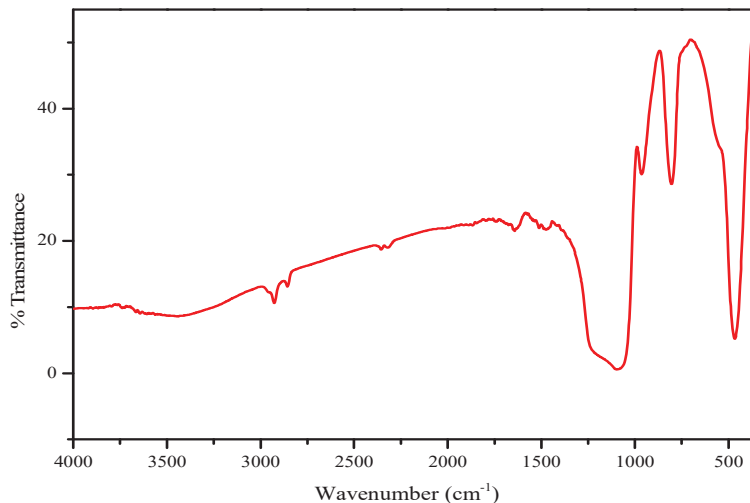


FIGURE 2. FTIR Spectrum mesoporous silica MCM-48

Effect of Contact Time

The contact time affected the adsorption balance of the congo red dye at a constant congo red dye concentration of 229.93 mg L^{-1} . The amount of congo red dye adsorbed on MCM-48 increased with the longer the contact time between the adsorbent and the adsorbate until the optimum time was reached. After reaching the optimum time, the amount of adsorbed congo red dye decreased. From minute 3 to minute 25 there was an increase for MCM-48. This is due to the rapid diffusion due to the collision between MCM-48 and the congo red dye and at 30 to 40 minutes it decreased due to saturation of the adsorbent surface so that it could no longer absorb dyes. The optimum adsorption time of congo red by MCM-48 was 25 minutes [5],[25].

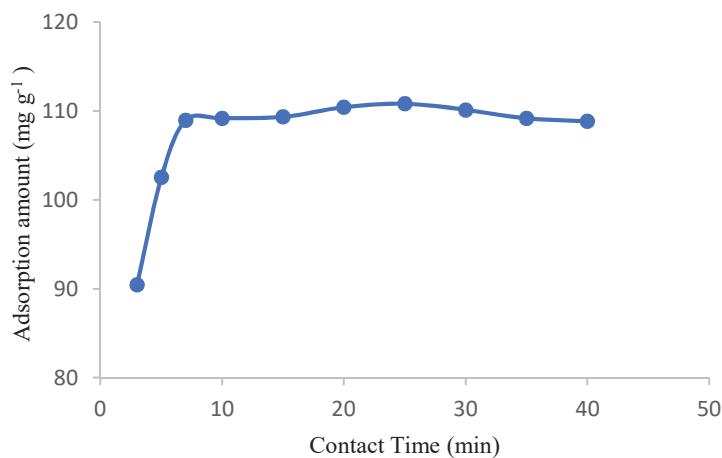


FIGURE 3. Effect of contact time on MCM-48

Kinetics Studies

The study of kinetic models allows a quantitative understanding of the adsorption process. The mechanism of the adsorption process can be explained very well with the help of kinetic models. In this study, pseudo first-order [26] and second-order pseudo [27] kinetics models were applied to study the adsorption mechanism of congo red dye. The first pseudo-order level equation used for solute adsorption from aqueous solution is Equation 4.

$$\ln(q_e - q_t) = -kt + \ln q_e \quad (4)$$

where q_e is the adsorption capacity at equilibrium (mg / g), q_t is the adsorption capacity at time t (mg / g), k is the kinetics constant. This pseudo-order adsorption can be calculated from a linear plot (figure 4a) of $\ln(q_e - q_t)$ Vs t (slope = K_1 , $q_e =$ intercept). The adsorption first-order pseudo-rate constants and the correlation coefficient values are summarized in Table 1 [28]. The pseudo-second order model is a kinetics model developed based on the complexation reaction between adsorbents and adsorbates. The equation for the rate of a pseudo-second-order reaction can be written in linear form as follows Equation 5.

$$\frac{t}{q_t} = \frac{1}{k_2 q_e^2} + \frac{1}{q_e} t \quad (5)$$

where k_2 is the rate constant of pseudo-second order ($\text{g/mg}^{-1} \cdot \text{min}^{-1}$). q_e and K_2 can be determined from the slope and the cut plot t/q against t is a linear curve with a slope of $1/q_e$ and an intercept of $1/k_2 q_e^2$ can be seen in Figure 4b. It can be concluded that for MCM-48 TC, MCM-48 C1 and MCM-48 C2 follow a pseudo second order kinetics model, which can be seen in Figure 4 and Table 1 [29].

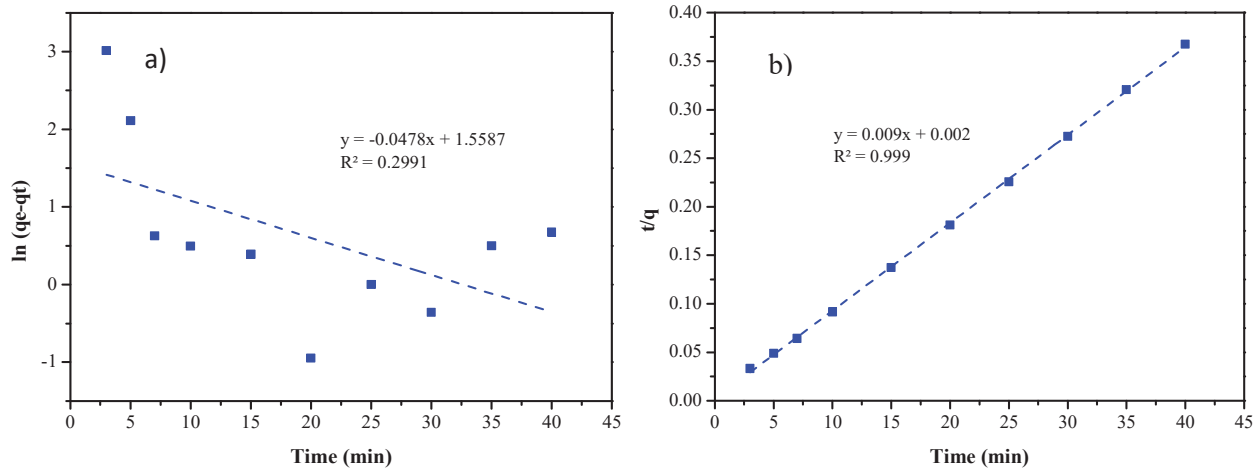


FIGURE 4. Kinetics model of MCM-48 a) pseudo-first order, b) pseudo-second order

TABLE 1. Kinetic parameters for the adsorption of the congo red dye on MCM-48

Adsorbent	pseudo-first order		pseudo-second order			
	K_1 (min^{-1})	R^2	q_e (mg/g)	K_2 ($\text{g} \cdot \text{mg}^{-1} \cdot \text{min}^{-1}$)	R^2	q_e (mg/g)
MCM-48	0.0478	0.299	36.199	0.039	0.999	109.890

Effect of Congo Red Concentration and Isothermal Adsorption

The adsorption capacity of congo red by MCM-48 can be determined by looking at the relationship between the concentration of congo red dye with a large amount of congo red adsorbed by MCM-48. The results obtained in this study for the adsorption capacity can be seen in Figure 5a). The concentration of the adsorbate solution affects the amount of congo red adsorbed by MCM-48. The higher the solution concentration, the more solute that can be adsorbed by the adsorbent. But the amount absorbed still increases until the highest concentration is used. Therefore, to determine the adsorption capacity of congo red by MCM-48, Langmuir and Freundlich's isothermal equations are

used. The adsorption isothermal curve can be seen in Figures 5b and c), respectively. By comparing the value of the least squares line (R^2), it will be known the appropriate adsorption isotherms for the adsorption of congo red dye by MCM-48. Adsorption of congo red by MCM-48 satisfies the Langmuir equation because the R^2 value for the Langmuir graph is close to 1 [20],[30].

TABLE 2. Congo red adsorption data based on Langmuir isothermal and Freundlich isothermal equations

Adsorbent	Langmuir isothermal			Freundlich isothermal		
	R^2	Q_0 (mg/g)	b (L/mg)	R^2	k (mg/g)	n (g/L)
MCM-48-C2	0.9943	185.185	0.0026	0.9599	67.1274	5.0327

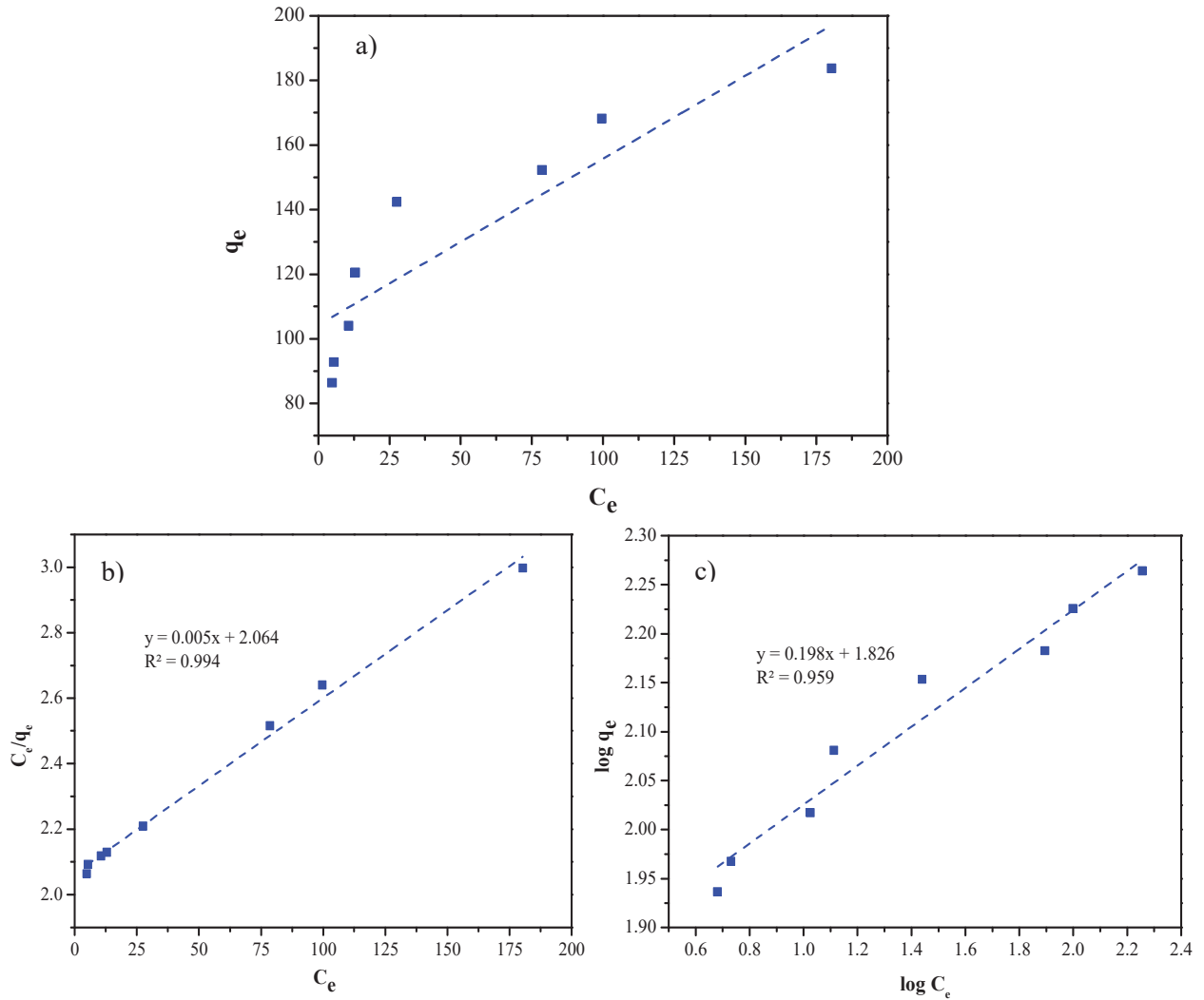


FIGURE 5. a) The effect of concentration on MCM-48, b) Langmuir isothermal, c) Freundlich isothermal

TABLE 3. Adsorption of the Congo Red dye using various types of adsorbents

Adsorbent	Adsorption Capacity (mg/g)	Reference
ZnO@Ze composite	161 (Langmuir)	[31]
Hexagonal Ni(OH) ₂ nanosheets	161.29 (Langmuir)	[27]
Chitosan Nanocomposite	1.8257 (Langmuir)	[32]
Onto antigonon leptopus leaf powder	18.18 (Langmuir)	[28]
Brewer's spent grain	36.5 (Langmuir)	[5]
Cellulosa from sago fround	15.63 (Langmuir)	[20]
Reagent NiO	39.7 (Langmuir)	[33]
Hierarchical Ni(OH) ₂ nanosheets	151.7 (Langmuir)	[33]
Hierarchical NiO	82.9 (Langmuir)	[33]
Al ₂ O ₃ -ZrO ₂	57.50 (Langmuir)	[34]
MCM-48	185.18 (Langmuir)	This work

Comparison of various adsorbents Table 3 compares the adsorption capacities of various types of adsorbents used to remove congo red dyes. The most important parameter to compare is the Langmuir Q_0 value because it is a measure of the adsorption capacity of the adsorbent. The value of Q_0 in this study is greater than in most of the previous works. This shows that congo red can easily be adsorbed on the MCM-48 mesopore silica. The results showed that MCM-48 could be considered a promising adsorbent for removing congo red from aqueous solutions.

CONCLUSION

Based on the research and data obtained, it can be concluded that the MCM-48 mesoporous silica is used to remove congo red anionic dye. The structure and texture properties of the synthesized materials were also studied by FTIR and SEM. The optimum adsorption time of congo red by MCM-48 was 25 minutes. Adsorption of congo red by MCM-48 follows a pseudo second order equation with the rate constant (k_2) obtained is 0.039 g/mg.min. The adsorption of congo red by MCM-48 is accordance with the Langmuir isothermal model with the value of the adsorption capacity obtained, namely 185.185 mg/g.

ACKNOWLEDGEMENTS

The author thanks Allah SWT, parents, family, friends as well as to the Leaders and Staff of the Chemistry Laboratory of FMIPA Unhas for their support in this research.

REFERENCES

1. M. Cheng, G. Zheng, D. Huang, C. Lai, Y. Liu, C. Zhang, R. Wang, L. Qin, W. Xue, B. Song, S. Ye and H. Yi, *J. Colloid Interface Sci.* **515**, 232-239 (2018).
2. N. El Messaoudi, M. El Khomri, A. Dbik, S. Bentahar, A. Lacherai and B. Bakiz, *J. of Environmental Chemical Engineering.* **4**, 3848-3855 (2016).
3. F. Deniz and R. A. Kepekci, *J. Microchemical.* **132**, 172-178 (2017).
4. Y. Y. Lau, Y. S. Wong, T. T. Teng, N. Morad, M. Rafatullah and S. A. Ong, *Chemical Engineering.* **246**, 383-390 (2014).
5. H. A. Chanzu, J. M. Onyari and P. M. Shiundu, *J. Hazard Mater.* **380**, 120897 (2019).
6. M. Foroughi-Dahr, H. Abolghasemi, M. Esmaili, A. Shojamoradi and H. Fatoorehchi, *Chemical Engineering Communications.* **202**, 181-193 (2014).
7. M. Shaban, M. R. Abukhadra, A. Hamd, R. R. Amin and K. Abde, *J. of Environmental Management.* **204**, 189-199 (2017).
8. V. Kumar, Y. Karnjkar, P. George, R. K. Singh and P. Chowdhury, *Chem. Pap.* **72**, 2055-2069 (2018).
9. H. Shayesteh, A. Ashra and A. Rahbar-kelishami, *J. Mol. Struct.* **1149**, 199-205 (2017).
10. I. Ali, O. M. L. Alharbi, Z. A. Allothman and A. Alwarthan, *Colloids Surfaces B Biointerfaces.* **171**, 606-613 (2018).
11. E. A. Burakova, P. T. Dyachkova, A. V. Rukhov, N. E. Tugolukov, E. V. Galunin, A. G. Tkachev, A. Arsh and I. Ali, *J. Mol. Liq.* **253**, 340-346 (2018).
12. L. Guz, G. Curutchet, M. R. Torres Sánchez and R. Candal, *J. Environ. Chem. Eng.* **2**, 2344-2351 (2014).

13. J. S. Beck, J. C. Vartuli, W. J. Roth, M. E. Leonowics, C. T. Kresge, K. D. Schmitt, C. T. W. Chu, D. H. Olson, E. W. Sheppard, S. B. McCullen, J. B. Higgins and J. L. Schlenker, *J. Am. Chem. Soc.* **114**, 10834-10843 (1992).
14. S. R. Zhai, Y. J. Gong, Y. Zhang, F. Deng, Q. Luo, D. Wu and Y. H. Sun, *J. Chin. Chem. Soc.* **51**, 49-57 (2004).
15. R. Ryoo, S. H. Joo and S. Jun, *J. Phys. Chem. B.* **103**, 7743-7746 (1999).
16. R. Nejat, A. R. Mahjoub, Z. Hekmatian and T. Azadbakht, *RSC. Adv.* **5**, 16029–16035 (2015).
17. F. Wei, Z. Liu, J. Lu and Z. Liu, *Microporous and Mesoporous Materials.* **131**, 224–229 (2010).
18. P. Taba, Makara Sains, **12**, 120-125 (2008).
19. X. Guo and J. L. Wang, *J. Mol. Liq.* **296**, 111850 (2019).
20. W. I. Arnata, Suprihatin, F. Fahma, Richana and C. T. Suharti, *Poll Res.* **38**, 557-567 (2019).
21. M. Anbia and A. Ghaffari *J. Iran. Chem. Soc.* **8**, S67-S76 (2011).
22. H. Kim, K. Jang, P. Galebach, C. Gilbert, G. Tompsett, C. W. Conner, W. C. Jones and S. Nair, *J. of Membrane Science.* **427**, 293-302 (2013).
23. S. J. Olusegun and N. D. S. Mohallem *Environmental Pollution.* **260** 114019 (2020).
24. L. Pajchel and W. Kolodziejski *Mater. Sci. Eng. C.* **91**, 734–742 (2018).
25. M. Mobarak, E. A. Mohamed, A. Q. Selim, M. T. Eissa and M. K. Seliem, *J. of Molecular Liquids.* **273**, 68–82 (2019).
26. A. S. Eltaweil, M. H. Ali, E. M. El-Monaem and G. M. El-Subruiti, *Advanced Powder Tec.* **31**, 1253-1263 (2020).
27. B. Yan, J. Lan, Y. Li, Y. Peng, L. Shi and R. Ran, *Colloids and Surfaces A.* **598**, 124828 (2020).
28. V. Sri-Devi, B. Sudhakar, K. Prasad, S. P. Jeremiah and M. Krishna, *Materials*, **26**, 3197-3206.
29. A. M Jasim and M. A Abbas, *J. of Physics*, **1294**, 052015 (2020).
30. Z. Cheng, L. Zhang, X. Guo, X. Jiang dan T. Li, *J. Molecular and Biomolecular Spectroscopy*, **137**, 1126-1143 (2015).
31. S. Madan, R. Shaw, S. Tiwari and S. Kumar, *Appl. Surf. Sci.* **487**, 907-917 (2019).
32. J. Jumadi, A. Kamari, N. A. Rahim, S. T. S. Wong, S. N. M. Yusoff, S. Ishak, M. M. Abdulrasool and S. Kumaran, *J. of Physics.* **1397**, 1742-6596 (2019).
33. B. Cheng, Y. Le, W. Cai and J. Yu, *J. of Hazardous Materials.* **185**, 889-897 (2011).
34. A. O. Adesina, A. E. Okoronkwo, N. D. S. Mohallem and S. J. Olusegun, *Environ. Technol.* 1-10 (2019).